Proceedings of the 3rd Croatian Conference on Earthquake Engineering - 3CroCEE
19–22 March 2025, Split, Croatia

DOI: https://doi.org/10.5592/CO/3CroCEE.2025.14

ANALYSIS OF SGM DATA CHARACTERISTICS FOR BETTER EXPLANATION OF BUILDING DAMAGE DURING THE FEB.6TH, 2023 KAHRAMANMARAS, TURKEY EARTHQUAKES

Oguz Koz [(1)], Sinem Guntepe [(2)], Oguz C. Celik [(3)]

[(1)] *Research Assistant, Structural and Earthquake Engineering Unit, Faculty of Architecture, Istanbul Technical University, Istanbul, Turkey, oguz.koz@itu.edu.tr*
[(2)] *Research Assistant, Structural and Earthquake Engineering Unit, Faculty of Architecture, Istanbul Technical University, Istanbul, Turkey, sinem.guntepe@itu.edu.tr*
[(3)] *Professor, Structural and Earthquake Engineering Unit, Faculty of Architecture, Istanbul Technical University, Istanbul, Turkey; celikoguz@itu.edu.tr*

Abstract

On February 6th, 2023, two massive earthquake doublet, with magnitudes of M_w 7.8 in Pazarcik and M_w 7.6 in Elbistan/Ekinozu, struck the southeastern region of Turkey, causing widespread devastation across multiple cities, resulting in human causalities over fifty thousand, and a total collapse of approximately thirty-three thousand buildings. This study presents a comprehensive analysis of strong ground motion (SGM) data characteristics to explain such extensive structural damage observed during the latest 2023 Kahramanmaras earthquakes. Key ground motion parameters, such as peak ground acceleration, peak ground velocity, peak ground displacement, effective duration, Arias intensity, and Housner intensity, were obtained using the SGM data of the selected stations in the region. Additionally, acceleration-displacement response spectra and inelastic earthquake spectra are generated for various damping ratios and ductility levels for several cities that were primarily affected by these earthquakes. The spectral values are compared with the design earthquake spectra provided by both past and current Turkish Seismic Codes. Relationship between earthquake source parameters and structural damage caused by these earthquakes is investigated. Particularly in regions where reports of substantial building damage were prevalent, the comparison revealed substantial discrepancies between the observed spectrum demands and the code-based design spectra. Results indicate that the recorded ground motions exceeded the recommended seismic reaction limits outlined in the Turkey Building Earthquake Code (TBEC, 2018), particularly for buildings with lower heights and fundamental periods less than 2 seconds. The peak accelerations were considerably high, resulting in considerable structural damage, particularly in structures with substandard columns (i.e. columns with high axial load and shear demands). Inelastic response spectra of buildings with shorter periods showed large fluctuations, suggesting that these structures are vulnerable to severe shaking.

Keywords: Turkey Earthquake Doublet, Strong Ground Motion, Characteristics, Inelastic response spectra.

1. Introduction

The M_w 7.8 and M_w 7.6 Kahramanmaras earthquake doublet (note that these magnitudes are alternatively given to be 7.9, 7.8, 7.7, and 7.5 in some sources) occurred on February 6th, 2023, in SE Turkey and NW Syria where, the Anatolian, Arabian, and African plates meet [1]–[5]. The M_w 7.8 rupture initiated on a previously unmapped splay fault extending southward from the main strand of the East Anatolian Fault Zone (EAFZ) at 04:17:34 local time (37.226°N, 37.014°E, 10 km deep, at 01:17:34.332 UTC). Approximately, nine hours later at 13:24:48 local time (10:24:49.640 UTC), a second large earthquake (Ekinozu earthquake, M_w 7.6), occurred with hypocentral parameters (38.011°N, 37.196°E, 7.4 km deep), along the northern strand of the EAFZ [5]–[7]. Compared to the North Anatolian Fault Zone (NAFZ), another significant fault line in Turkey that has produced major earthquakes for a long time such as the 1999 Kocaeli (M_w=7.4) Earthquake and 1999 Duzce Earthquake (M_w=7.1) and 2022 Duzce (Golyaka) Earthquake (M_w=6.1) while the EAFZ has historically exhibited lower seismic activity, with only a few earthquakes exceeding M_w 7.0 in recent decades. However, it was well known that the EAFZ is capable of producing significant earthquakes, as evidenced by events

DOI: https://doi.org/10.5592/CO/3CroCEE.2025.14

in 1513, 1795, and others that occurred between 1822 and 1905 [8]. The most significant event before the 2023 Kahramanmaras sequence was the M_w 6.8 Doganyol-Sivrice earthquake on January 24th, 2020, which also caused widespread building damage and total collapses in the region [9]. The EAFZ serves as a major plate boundary accommodating the westward extrusion of the Anatolian plate toward the Aegean Sea. Despite its relatively quiet seismic history, this fault system has been the source of destructive earthquakes throughout recorded history, as documented by several studies [8], [10].

The 2023 earthquake sequence is distinguished as the most devastating and recorded event along the EAFZ in recent history, exceeding the impacts of previous earthquakes such as the 1971 Bingol (M_w 6.6), the 2003 Bingol (M_w 6.4), 2010 Kovancilar, Elazig (M_w 6.1), and the 2020 Doganyol-Sivrice earthquakes, as reported by USGS. The region affected by the February 6th, 2023 earthquakes experienced over 50,000 casualties and significant structural devastation across 11 city centers and their districts. Following the mainshock, a series of large aftershocks, including a M_w 6.6 event near Nurdagi, Gaziantep, and more than 30 moderate-sized earthquakes (M_w 5.0~6.0), further damaged already compromised structures. In the three months following the disaster, over 33,000 aftershocks of varying magnitudes were recorded, highlighting the seismic complexity of the region [16].

Structural damage observed during the past earthquakes was influenced by various factors, including poor material quality, inadequate reinforcement, irregular architectural configurations, poor soil conditions, and non-compliance with seismic/building regulations [11]–[15]. Findings from studies on the latest Kahramanmaras earthquake sequence revealed comparable/expected patterns of structural failure in existing buildings [4]. In urban areas, most of the affected structures were reinforced concrete (RC) buildings, while rural regions predominantly comprised masonry (mostly rubble stone) or hybrid constructions incorporating traditional timber frames with mortar binders. The destruction also included cultural and religious landmarks, with many historic mosques, churches, and minarets sustaining severe damage or collapse. Poor soil conditions (amplifications, liquefaction etc.) had also a negative impact in the seismic behavior of buildings especially at Antakya (Antioch), Kahramanmaras, Iskenderun, and Golbasi (Adiyaman).

The aim of this study is to develop a comprehensive analysis of the characteristics of the strong ground motion data in order to possibly explain the widespread structural damage observed during the 2023 Kahramanmaras earthquakes. Spectral characteristics are obtained and compared for the three most affected cities (Kahramanmaras, Hatay, and Malatya) with each city experiencing damage to over 50% of its buildings. The study establishes an evaluation of seismic parameters, offering a deeper understanding of the factors contributing to observed structural damage.

This study underscores the critical role of spectral characteristics in understanding structural damage/collapses observed in buildings during the 2023 Kahramanmaras, Pazarcik and Elbistan/Ekinozu earthquakes. It is concluded that high PGA and PGV values were linked to severe damage as expected, and notable discrepancies are found between spectral demands and the TBEC (2018) design spectra, especially for low-to- midrise structures.

2. Analysis of Strong Ground Motions

2.1. Strong ground motion data

This work delves into earthquake records from the four provinces with the most heavily damaged structures during the 2023 Kahramanmaras earthquakes, including Kahramanmaras, Hatay, Malatya, and Adiyaman. All data were downloaded from TADAS AFAD [16]. Since the available AFAD data were unprocessed, a filtering was applied to remove noise-contaminated frequency content from the records while preserving the primary ground motion characteristics within the predefined frequency band. For this purpose, a fourth-order Butterworth noncausal filter was utilized. The filtering range was determined based on a literature review of studies on the 2023 Kahramanmaras earthquakes and visual inspections of the Fourier Amplitude Spectrum [2]. Strong ground motion records from stations 0201, 3146, and 4632 of the Pazarcik earthquake, as well as 0213, 4414, and 4631 of the Elbistan/Ekinozu earthquake, were found to be interrupted and therefore excluded from the evaluation. Although

Proceedings of the 3rd Croatian Conference on Earthquake Engineering - 3CroCEE
19–22 March 2025, Split, Croatia

DOI: https://doi.org/10.5592/CO/3CroCEE.2025.14

Adıyaman had the highest ratio of collapsed buildings relative to its building stock, the acceleration records from the stations in the region were excluded from the analysis due to interruptions in the data. Processed data were used to compute key parameters, including Peak Ground Acceleration (PGA), Peak Ground Velocity (PGV), Peak Ground Displacement (PGD), Arias Intensity (AI), Housner Intensity (HI or a.k.a. SI), and Effective Duration (5-95%). The definitions and equations of earthquake parameters are summarized in Table 1.

Table 1. Definitions and Equations of Earthquake Characteristics.

Earthquake Characteristic	Definition	Equation
Peak Ground Acceleration PGA	Maximum ground acceleration during an earthquake	$\max\lvert a(t)\rvert$
Peak Ground Velocity PGV	Maximum ground velocity during an earthquake.	$\max\lvert v(t)\rvert$
Peak Ground Displacement PGD	Maximum ground displacement during an earthquake.	$\max\lvert d(t)\rvert$
Arias Intensity AI	A measure of earthquake energy per unit weight absorbed by an idealized oscillator over the earthquake duration (T_d).	$AI = \frac{\pi}{2g}\int_0^{T_d}[a(t)]^2dt$
Housner Intensity HI	Response spectrum intensity, calculated as the integral of pseudo spectral velocity over the 0.1~2.5s period range for a 5% damping ratio (ξ).	$SI(\xi) = \int_{0.1}^{2.5} S_{pv}(\xi,t)\ dt$
Effective Duration (5-95%)	The time interval between the points at which 5% and 95% of the total energy has been recorded.	$t_{eff} = t_{95} - t_5$

2.2. Earthquake Characteristics and Observations

An earthquake's damage potential can be assessed by using ground motion parameters, each reflecting different physical characteristics of seismic activity. Peak Ground Acceleration (PGA) is one of the most well-known and commonly used indicators in seismic design. However, it does not account for the duration or frequency content of the earthquake and is more suitable for structures with short periods (T < 0.3 s) [17]. Peak Ground Velocity (PGV) represents the maximum ground velocity during an earthquake. It is particularly important for evaluating the dynamic response of flexible structures and provides insights into the earthquake's magnitude and intensity. Peak Ground Displacement (PGD), on the other hand, correlates with damage in long-period structures, including both buildings and infrastructure. Arias Intensity (AI) and Housner Intensity (HI) are energy-based parameters that consider the duration and frequency content of the ground motion. Housner Intensity focuses on dynamic demands in structures with periods between 0.1 and 2.5 seconds. Finally, effective duration represents the time interval during which 5% to 95% of the cumulative energy (Arias Intensity) is released. A longer effective duration indicates that structures are subjected to a greater number of seismic load cycles, which increases the probability of structural damage due to the accumulation of damage caused by repeated loading.

The strong ground motion characteristics from selected stations in the three provinces with the highest damage during the Pazarcik and Elbistan/Ekinozu earthquakes are presented in Tables 2 and 3, respectively. For the Pazarcik earthquake, the analyzed stations include Kahramanmaras (4614), Malatya (4404), and Hatay (3129), while for the Elbistan/Ekinozu earthquake, the selected stations are Kahramanmaras (4612), Malatya (4406), and Hatay (3144).

Table 2. Ground Motion Characteristics for the M_w 7.8 Pazarcik Earthquake.

Station Code	PGA (cm/sec²)	PGV (cm/sec)	PGD (cm)	PGA$_D$ (cm/sec²)	PGA/PGA$_D$	AI (m/sec)	HI (cm)	Effective duration 5~95%
3129 E-W	1203.7	68.8	53.3	438.0	2.75	18.3	286.6	15.3
3129 N-S	1366.1	172.5	37.6	438.0	3.12	25.0	545.5	10.7
3129 U-D	797.5	42.9	22.1	350.4	2.28	6.9	165.3	10.6
4614 E-W	2179.8	61.9	26.7	441.4	4.94	58.7	164.6	23.8
4614 N-S	1984.1	85.5	57.9	441.4	4.50	88.2	205.8	23.1
4614 U-D	1602.8	37.4	24.2	353.1	4.54	36.4	97.4	21.0
4404 E-W	139.7	11.4	7.8	495.1	0.28	0.2	39.4	22.0
4404 N-S	132.8	13.6	12.8	495.1	0.27	0.2	42.1	21.2
4404 U-D	96.7	11.9	4.8	396.0	0.24	0.1	34.8	29.3

Table 3. Ground Motion Characteristics for the M_w 7.6 Elbistan/Ekinozu Earthquake.

Station Code	PGA (cm/sec²)	PGV (cm/sec)	PGD (cm)	PGA$_D$ (cm/sec²)	PGA/PGA$_D$	AI (m/sec)	HI (cm)	Effective duration 5~95%
3144 E-W	76.1	11.3	10.6	464.2	0.16	0.1	29.5	31.4
3144 N-S	59.7	8.1	5.6	464.2	0.13	0.1	23.8	31.3
3144 U-D	27.5	4.1	4.6	371.4	0.07	0.0	15.8	47.7
4406 N-S	471.5	20.2	11.8	419.1	1.13	3.3	94.5	18.4
4406 E-W	409.1	33.8	17.2	419.1	0.98	2.9	97.8	17.4
4406 U-D	303.1	19.9	9.6	335.3	0.90	1.4	62.5	17.0
4612 N-S	637.3	166.7	63.6	377.9	1.69	4.2	410.6	20.2
4612 E-W	523.7	73.3	42.8	377.9	1.39	3.2	315.1	28.8
4612 U-D	488.3	54.3	30.6	302.3	1.62	1.8	129.6	12.0

In the Pazarcik earthquake, the maximum ground acceleration recorded at station 4614 (N-S) exceeded 2000 cm/s², representing a significant seismic event and never recorded in Turkey's history. High vertical acceleration values further increased the axial loads on columns with already high axial force demands (even under gravity loading due to poor concrete quality) and insufficient ductility stemming from poor rebar detailing, contributing to brittle failures in these structures. In Malatya, which experienced significant building damage, the maximum PGA at the 4404 station during the Pazarcik earthquake was relatively low, recorded to be 140 cm/s², with a Housner Intensity of 42.1 cm. However, in the Elbistan/Ekinozu earthquake, the PGA increased significantly to 471.5 cm/s², and the Housner Intensity reached 97.8 cm. These evaluations indicate that the Elbistan/Ekinozu earthquake was more destructive in Malatya in terms of energy release. Long earthquake durations observed across multiple stations, highlight the significant role of prolonged seismic excitation in amplifying cumulative damage (or damage growth), particularly in structures with inadequate detailing or insufficient energy dissipation capacity.

DOI: https://doi.org/10.5592/CO/3CroCEE.2025.14

To better provide a comparative perspective, the Housner Intensity (HI) values from the 1999 Duzce (M_w 7.1), 1999 Kocaeli (M_w 7.4), and 2011 Van (M_w 7.0) earthquakes offer valuable context for evaluating the ground motion characteristics of the 2023 Kahramanmaras earthquakes. For instance, the HI values during the 1999 Kocaeli earthquake reached up to 335 cm, while the 1999 Düzce and 2011 Van earthquakes recorded maximum values of 269 cm and 146 cm, respectively. In contrast, the HI values computed for the 2023 Kahramanmaras earthquakes are significantly higher as shown in Tables 2 and 3. During the Pazarcik event, the HI value at Hatay (3129 N-S component) reached 545.5 cm, while Kahramanmaras (4614 N-S component) recorded 205.8 cm. Similarly, during the Elbistan/Ekinozu event, Malatya (4612 N-S component) resulted in an HI value of 410.6 cm. These remarkable differences highlight the exceptionally high energy demands imposed by the 2023 Kahramanmaras earthquake sequence, particularly on short-to-medium period structures (0.1~2.5 seconds).

3. Spectral Characteristics and Structural Damage Relation

In the earthquake-stricken area, 86.7% of buildings are made with reinforced concrete while 2.4% of the buildings are steel, 3.5% are masonry, and 3.6% are prefabricated [18]. The other category includes timber, mixed or unidentified structural systems and the percentages of other structural systems is quite low. Structural damage classification categorizes buildings based on the severity of earthquake-induced damage, ranging from slight damage to totally collapsed buildings. Slightly damaged buildings exhibit minor cracks on paint, plaster, or walls, with some localized plaster detachment due to the earthquake. Moderately damaged buildings show wall fractures (nonstructural) and minor cracks in structural members, making them uninhabitable without prior repair or structural strengthening. Heavily damaged buildings experience extensive and widespread flexural or shear failures or separation of structural elements, resulting in an irreparable loss of structural integrity, both in terms of strength and economic efficiency. Urgent demolition is required for buildings where substantial permanent deformations have occurred in load-bearing components, leading to partial or total structural collapses. In terms of the building's assessment by Ministry of Environment, Urbanization, and Climate Change of Turkey on 2,457,942 buildings, there were 38,440 collapsed buildings and 20,537 were in need of urgent demolition, 204,745 of them got severe damage, 41,732 experienced moderate damage, and 636,840 were scored as slightly damaged [19]. The number of total and damaged buildings for the most affected 4 cities from these earthquakes is given in Table 4. The distribution of damage to buildings in these four cities is also displayed in Figure 1. Various levels of structural damage observed in buildings in the province of Kahramanmaras are presented in Figure 2.

Table 4. Number of Damaged Buildings for the Most Affected 4 Cities [19].

City	Total Number of Buildings	Slight Damage	Moderate Damage	Severe Damage	Urgent Demolition	Collapsed
Adiyaman	120,496 (100%)	39,888 (33.10%)	4,493 (3.73%)	20,481 (17.00%)	2,271 (1.88%)	6,062 (5.03%)
Hatay	406,849 (100%)	114,566 (28.16%)	12,630 (3.10%)	54,960 (13.51%)	8,839 (2.17%)	13,345 (3.28%)
Kahramanmaras	243,153 (100%)	81,134 (33.37%)	6,036 (2.48%)	35,691 (14.68%)	4,432 (1.82%)	7,480 (3.08%)
Malatya	178,987 (100%)	51,933 (29.01%)	2,323 (1.30%)	35,368 (19.76%)	1,746 (0.98%)	5,545 (3.10%)

DOI: https://doi.org/10.5592/CO/3CroCEE.2025.14

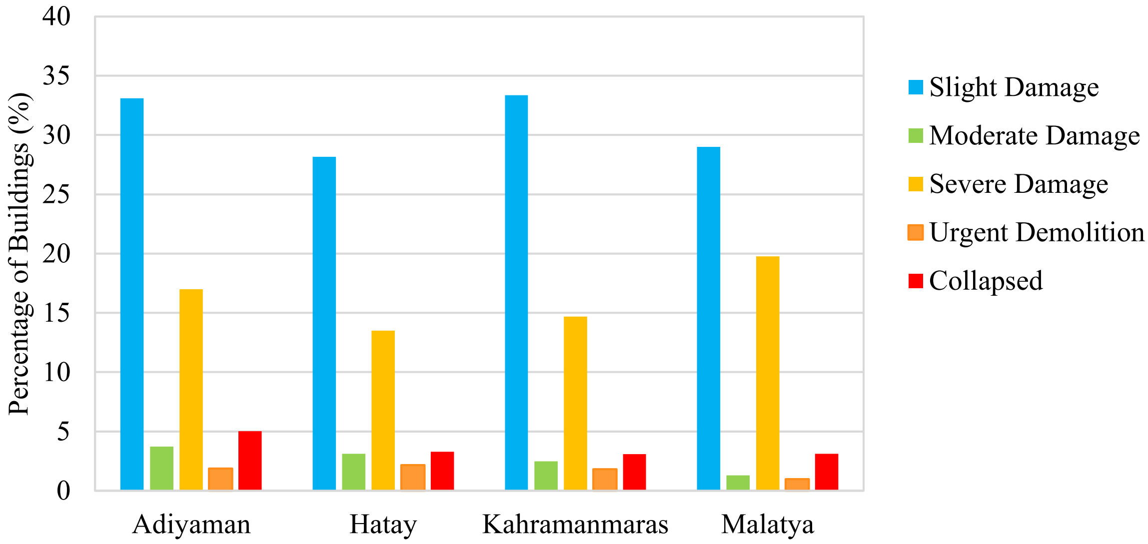

Figure 1. Building Damage Distribution (%) in the Most Affected Cities

Figure 2. Damaged building images from the province of Kahramanmaras

Acceleration, velocity, and displacement spectra were generated for the stations with the maximum recorded accelerations in the three provinces with the highest rate of damaged building stock—Hatay, Kahramanmaras, and Malatya. Horizontal and vertical accelerations, velocity, and displacement spectra were computed for systems with 5% damping and are presented in Figures 3, 4, and 5. Additionally, the acceleration spectra corresponding to the ground motion levels with a 2% probability of exceedance in 50 years (return period of 2475 years, DD1) and the design earthquake level with a 10% probability of exceedance in 50 years (return period of 475 years, DD2) are illustrated. These earthquake levels are plotted for the weakest soil conditions, classified as ZE soil class (e.g., loose sand, gravel, or soft to firm clay layers).

In Turkey Building Earthquake Code (2018), the vertical elastic design spectrum is also defined. The design accelerations for DD1 and DD2 earthquake levels are illustrated on the vertical earthquake (U-D) acceleration spectrum. To enhance the clarity of the design spectrum levels, the vertical axis of the acceleration spectra was capped at 3g. However, in the figure illustrating the inelastic spectra (Fig. 7.a), the maximum points are displayed without being capped.

A significant portion (37%) of the existing building stock in the earthquake-affected region was constructed before 1998 and was therefore subjected to the earthquake code in effect at that time [18]. Between 1975 and 1998, Specifications for Structures to be Built in Disaster Zones (SSBDZ, 1975) were in use. Consequently, the design acceleration spectrum from this code has also been included in the acceleration spectra for comparison.

In the elastic response spectrum, within the period range T=0~0.5 s, the spectral acceleration of the 4614 N-S component peaked at 7.4g, while the 3129 N-S component reached its highest value at 5.32g. This highlights the significant impact of high-frequency ground motions on short-period structures (such as single-story or low-rise buildings), which were more vulnerable to these effects.

The spectral values obtained from the acceleration records measured at the Kahramanmaras 4614 and Hatay 3129 stations were found to significantly exceed the design acceleration spectrum, particularly in the short-period range. In Malatya, while the accelerations caused by the Pazarcik earthquake remained below the design spectrum, the accelerations generated during the Elbistan/Ekinozu earthquake exceeded the design spectrum values. High PGA values are indicative of intense shaking and immediate structural demands but are insufficient to comprehensively explain structural damage. Other factors contributing to structural damage include the earthquake's duration, directionality, and frequency content; the characteristics of the building stock; local soil conditions; architectural and structural design flaws in the load-bearing systems; and issues arising from non-compliance with the construction design or errors during the construction phase.

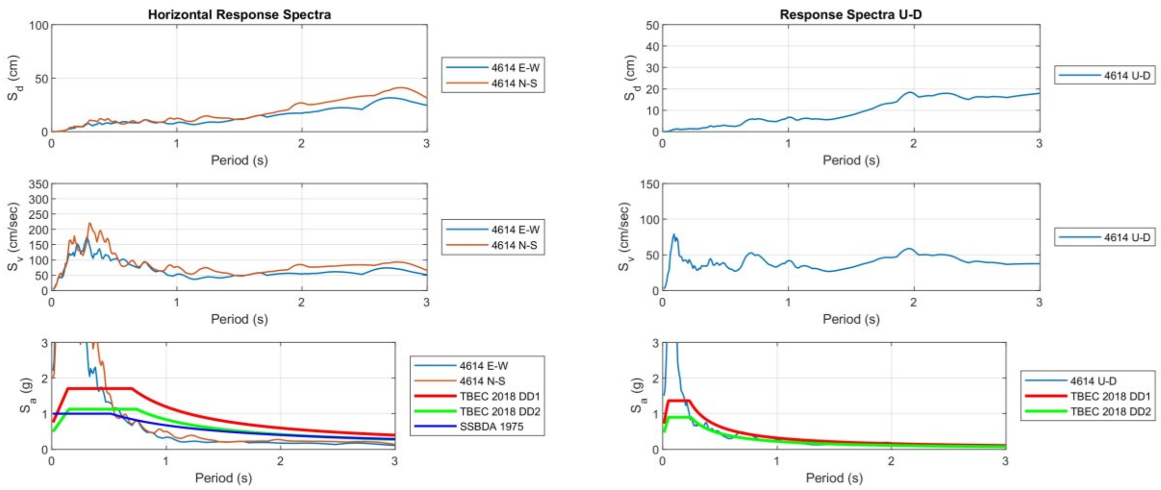

Figure 3. Response spectra for Kahramanmaras stations during the Pazarcik Earthquake:
(a) Horizontal components, (b) Vertical component

DOI: https://doi.org/10.5592/CO/3CroCEE.2025.14

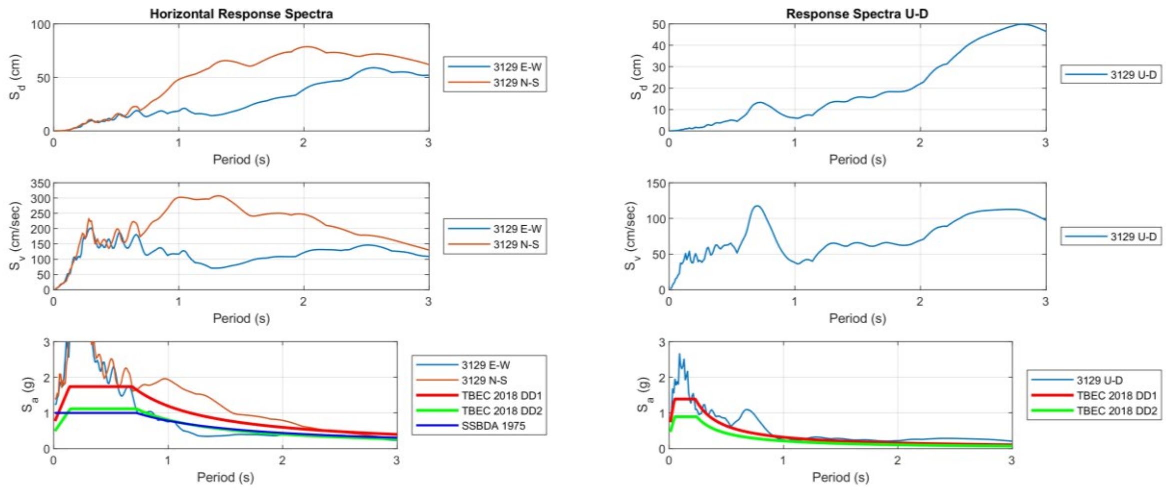

Figure 4. a) Response spectra for Hatay stations during the Pazarcik Earthquake:
(a) Horizontal components, (b) Vertical component

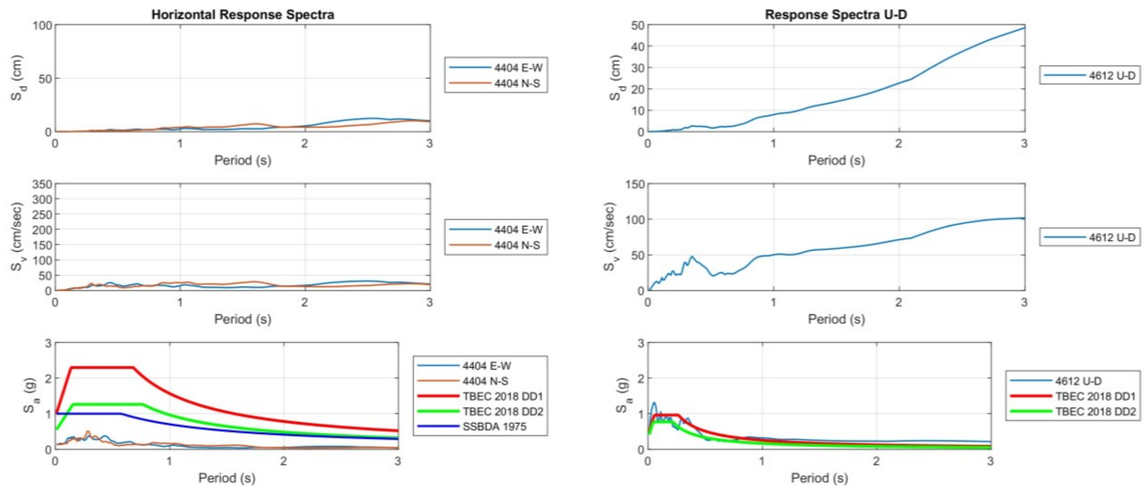

Figure 5. Response spectra for Malatya stations during the Elbistan/Ekinozu Earthquake:
(a) Horizontal components, (b) Vertical component

The Acceleration-Displacement Response Spectrum (ADRS) is a tool used in structural engineering to understand how buildings or other structures react to dynamic forces like earthquakes or explosions. It visually compares maximum acceleration and displacement, providing insights into how a structure might behave under different levels of ground motion [20]. By analyzing the intersection of the demand curve (ground motion) and the capacity curve (structural response), engineers identify the structure's performance point. This helps determine if the structure can withstand the applied forces without damage or if it faces a risk of failure. ADRS is crucial in seismic design and performance-based evaluations to ensure structural safety under dynamic loading conditions.

Elastic acceleration-displacement response spectra (bi-spectra) were generated for the Kahramanmaras 4614 and Hatay 3129 stations during the Pazarcik earthquake, as well as the Malatya 4612 station during the Elbistan/Ekinozu earthquake, and are presented in Figure 6.

Proceedings of the 3rd Croatian Conference on Earthquake Engineering - 3CroCEE
19–22 March 2025, Split, Croatia

DOI: https://doi.org/10.5592/CO/3CroCEE.2025.14

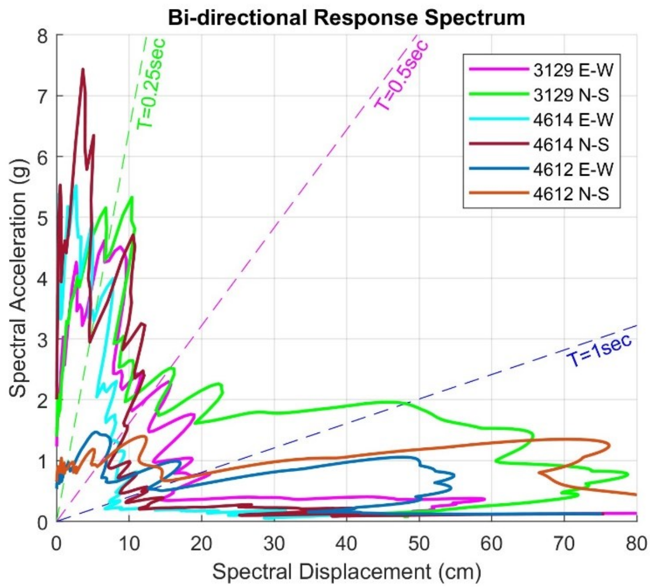

Figure 6. Acceleration-displacement response spectra (bi-spectra)

Constructing inelastic response spectra is useful in seismic engineering to account for yielding in structures during strong shaking. The ductility factor, μ, is defined as the ratio of maximal inelastic deformation to yield deformation, acting as a crucial indicator of a structure's capacity to endure substantial plastic deformation while preserving its stability. The displacement ductility factor (μ) is utilized as a parameter for generating the inelastic response spectrum. Elastic structures are assigned a value of μ=1, whereas systems with high ductility can be considered to have μ=8. The response modification factor (R) is a seismic design parameter and a proportional ductility factor, that represents the inelastic behavior of a structure [21]. The value of R is influenced by various parameters, including the height of the structure, as high-rise and low-rise structures respond differently to seismic forces. Building codes provide well-defined R-values for various structural systems and materials [22]. According to the Turkey Building Earthquake Code (TBEC-2018), the R-value for RC framed buildings with a high level of ductility is specified to be 8. For buildings combining frames with RC shear walls (dual systems), R is given to be 7. Similarly, R is taken to be 8 for steel frame buildings with high ductility, and for reinforced masonry structures, R=4. Figure 7 illustrates the elastic response spectra (μ=1) and inelastic response spectra for ductility levels μ=2, 4, and 8, derived from seismic recordings at three stations (Kahramanmaras (4614), Malatya (4612), and Hatay (3129) [23]). Even with increased ductility ratios, the persistently high acceleration demands observed in the inelastic spectra for short-period structures (T<0.5 s) indicate that these structures dissipate a significant portion of the seismic energy through acceleration, highlighting their limited plastic deformation capacity. The significant reduction in acceleration demands for long-period structures (T>1 s) highlights their ability to effectively dissipate seismic energy through deformation due to their ductile behavior.

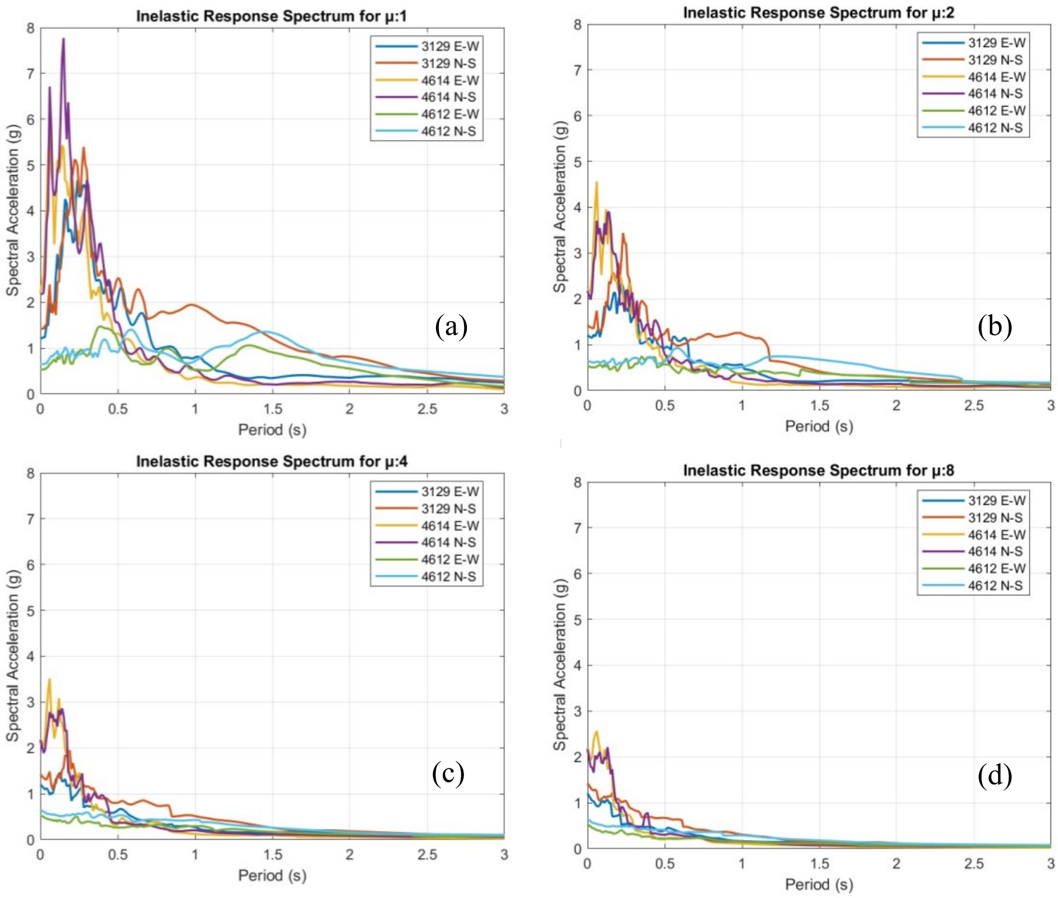

Figure 7. a) Elastic response spectra (μ = 1), b) Inelastic response spectra for μ = 2, c) Inelastic response spectra for μ = 4, and d) Inelastic response spectra for μ = 8

4. Conclusions

This study highlights the significance of strong ground motion characteristics in better explaining the structural vulnerabilities evident during the February 6th, Kahramanmaras (Pazarcik&Elbistan/Ekinozu) earthquake sequence. Ground motion parameters such as PGA, PGV, Arias Intensity, and Housner Intensity, were examined, and their effects on structural damage were evaluated by comparisons with the TBEC (2018) design spectra. The following results can be deduced from this work:

- High PGA values are directly connected with areas of significant building damage.
- Notable differences were identified between the spectral demands and the TBEC (2018) design spectra, particularly in case of low-to-midrise structures.
- The Housner Intensity values revealed a significant energy demand for short-period structures, suggesting potential deficiencies even in code-compliant designs.
- The effective duration of shaking was identified as a contributing factor to cumulative damage and damage growth particularly in structures exhibiting inadequate/nonductile detailing.
- Although the PGA values in some regions exceeded the design earthquake spectra, it is believed that the majority of collapsed buildings (3~5% of the total building stock) were either not constructed in compliance with code requirements or were affected by factors such as structural irregularities and poor material strength.
- Poor soil conditions (amplifications, liquefaction etc.) had also a negative impact in the seismic behavior of buildings especially at Antakya (Antioch), Kahramanmaras, Iskenderun, and Golbasi (Adiyaman).

DOI: https://doi.org/10.5592/CO/3CroCEE.2025.14

References

[1] Wu, F.et al. (2023): Pulse-like Ground Motion Observed during the 6 February 2023 M_w 7.8 Pazarcik Earthquake (Kahramanmaraş, SE Türkiye). Earthq. Sci., 36, 4, 1–12, doi: https://doi.org/10.1016/j.eqs.2023.05.005

[2] Hu, J., Liu, M., Taymaz, T., Ding, L. and Irmak, T. S. (2024): Characteristics of strong ground motion from the 2023 M_w 7.8 and M_w 7.6 Kahramanmaraş earthquake sequence, *Bull. Earthq. Eng.*, doi: https://doi.org/10.1007/s10518-023-01844-2

[3] Goldberg, D. E. et al. (2023): Rapid Characterization of the February 2023 Kahramanmaraş, Türkiye, Earthquake Sequence. *Seism. Rec.*, 3, 2, 156–167, doi: https://doi.org/10.1785/0320230009

[4] Celik, O. C. Ulker MBC, Gocer C, Guntepe S, Koz O, Eyupgiller MM, et al. (2024): Multidisciplinary reconnaissance investigation covering structural, geotechnical, and architectural based damage to mid-rise residential buildings following the February 6th, 2023 Kahramanmaras earthquake doublets (M_w 7.8, M_w 7.6). *Soil Dyn. Earthq. Eng.*, 182, 108738, doi: https://doi.org/10.1016/j.soildyn.2024.108738

[5] Liu, C. et al. (2023): Complex multi-fault rupture and triggering during the 2023 earthquake doublet in southeastern Türkiye. *Nat. Commun.*, 14, 1, pp. 1–14, 2023, doi: https://doi.org/10.1038/s41467-023-41404-5

[6] United States Geological Survey (USGS), *M 7.8 - Pazarcik earthquake, Kahramanmaras earthquake sequence.* https://earthquake.usgs.gov/earthquakes/eventpage/us6000jllz/executive (accessed Aug. 26, 2023).

[7] United States Geological Survey (USGS), *M 7.5 - Elbistan earthquake, Kahramanmaras earthquake sequence.* https://earthquake.usgs.gov/earthquakes/eventpage/us6000jlqa/executive (accessed Aug. 29, 2023).

[8] Wang, Z., Zhang, W., Taymaz, T., He, Z., Xu, T., and Zhang, Z. (2023): Dynamic Rupture Process of the 2023 M_w 7.8 Kahramanmaraş Earthquake (SE Türkiye): Variable Rupture Speed and Implications for Seismic Hazard. *Geophys. Res. Lett.*, 50, 15, 1–11, doi: https://doi.org/10.1029/2023GL104787

[9] Celik, O.C., Bal, A., Atasever, K., Emanet, S., Koca, S. (2020): 24 Ocak 2020 Doğanyol (Malatya)-Sivrice (Elazig) Depreminden Gözlemler (M_w 6.7-Doğu Anadolu Fay Zonu). *Bet. Prefabrikasyon,* 134, April, 5–29.

[10] Emre, Ö. et al. (2018): Active fault database of Turkey. *Bull. Earthq. Eng.*, 16, 8, 3229–3275, 2018, doi: https://doi.org/10.1007/s10518-016-0041-2

[11] Celik, O.C., Cili, F. Ozgen, K. (2000): 17 Agustos 1999 Kocaeli (Izmit) Depremi'nden Gözlemler. *Yapi Dergisi (in Turkish).*

[12] Celep, Z., Erken, A., Taskin, B., and Ilki, A. (2011): Failures of masonry and concrete buildings during the March 8, 2010 Kovancilar and Palu (Elazig) Earthquakes in Turkey. *Eng. Fail. Anal.*, 18, 3, 868–889, 2011, doi: https://doi.org/10.1016/j.engfailanal.2010.11.001

[13] Yazgan, U., Oyguç, R., Ergüven, M. E., and Celep, Z. (2016): Seismic performance of buildings during 2011 Van earthquakes and rebuilding efforts, *J. Earthq. Eng. Eng. Vib.*, 15, 3, 591–606, doi: https://doi.org/10.1007/s11803-016-0346-9

[14] Tapan, M., Comert, M., Demir, C., Sayan, Y., Orakcal, K., and Ilki, A. (2013): Failures of structures during the October 23, 2011 Tabanli (Van) and November 9, 2011 Edremit (Van) earthquakes in Turkey. *Eng. Fail. Anal.*, 34, 606–628, 2013, doi: https://doi.org/10.1016/j.engfailanal.2013.02.013

[15] A. Yakut et al. (2022): Performance of structures in İzmir after the Samos island earthquake. *Bull. Earthq. Eng.*, 20, 14, 7793–7818, 2022, doi: https://doi.org/10.1007/s10518-021-01226-6

[16] Disaster and Emergency Management Presidency (AFAD).: *AFAD TADAS Website.* https://tadas.afad.gov.tr/map (accessed Dec. 14, 2024).

[17] Malcioglu, F.S., O'Kane, A., Donmez, K. and Aktas, Y.D. (2022): Characteristics of Strong Ground Motions in the 30 October 2020, M_W 6.9 Aegean Sea Earthquake. *Front. Built Environ.* 8:870279. doi: https://doi.org/10.3389/fbuil.2022.870279

DOI: https://doi.org/10.5592/CO/3CroCEE.2025.14

[18] Presidency of Strategy and Budget (2023): *2023 Kahramanmaras ve Hatay Earthquakes Report (in Turkish)* [Online]. Available: https://www.sbb.gov.tr/wp-content/uploads/2023/03/2023-Kahramanmaras-ve-Hatay-Depremleri-Raporu.pdf

[19] Damcı, E., Temür, R., Kanbir, Z., Şekerci, Ç., Köroğlu, E.Ö. (2025): Comprehensive Investigation of Damage Due to 2023 Kahramanmaraş Earthquakes in Türkiye: Causes, Consequences, and Mitigation (Pre-print), *J. Build. Eng.,* 99, 111420, doi: https://doi.org/10.1016/j.jobe.2024.111420

[20] Heath, D. J., Wilson, J. L., Gad, E. F. (2015): Acceleration-displacement response spectrum vibration limits for blast vibrations. *Australian Journal of Structural Engineering*, 16(1), 1-16. doi: https://doi.org/10.7158/13287982. 2015.11465175

[21] Heshmatollah, A., Hejazi, F., Jaafar, S.F. (2019): Response Modification Factor: Review Paper. *IOP Conf. Ser.: Earth Environ. Sci. 357 012003*, doi: https://doi.org/10.1088/1755-1315/357/1/012003

[22] Sadjadi, R. and Kianoush, M. R. (2010): Response Modification Factor for reinforced concrete (RC) Liquid Containing Structures. *Proceedings of the 9th U.S. National and 10th Canadian Conference on Earthquake Engineering*, Toronto, Ontario, Canada, pp. 3496–3505.

[23] Seismosoft. *SeismoSignal – A computer program for signal processing of strong-motion data.* 2011. Version 4.3 [software]. https://seismosoft.com/products/seismosignal/ (accessed Dec. 14, 2024).